AD-A067 703 NAVAL POSTGRADUATE SCHOOL MONTEREY CALIF F/G 20/4
DESIGN OF SHOCK-FREE TRANSONIC FLOW IN TURBOMACHINERY.(U)
NOV 78 H SOBIECZKY
UNCLASSIFIED NPS67-78-005 NL

1 OF 1
AD A067703

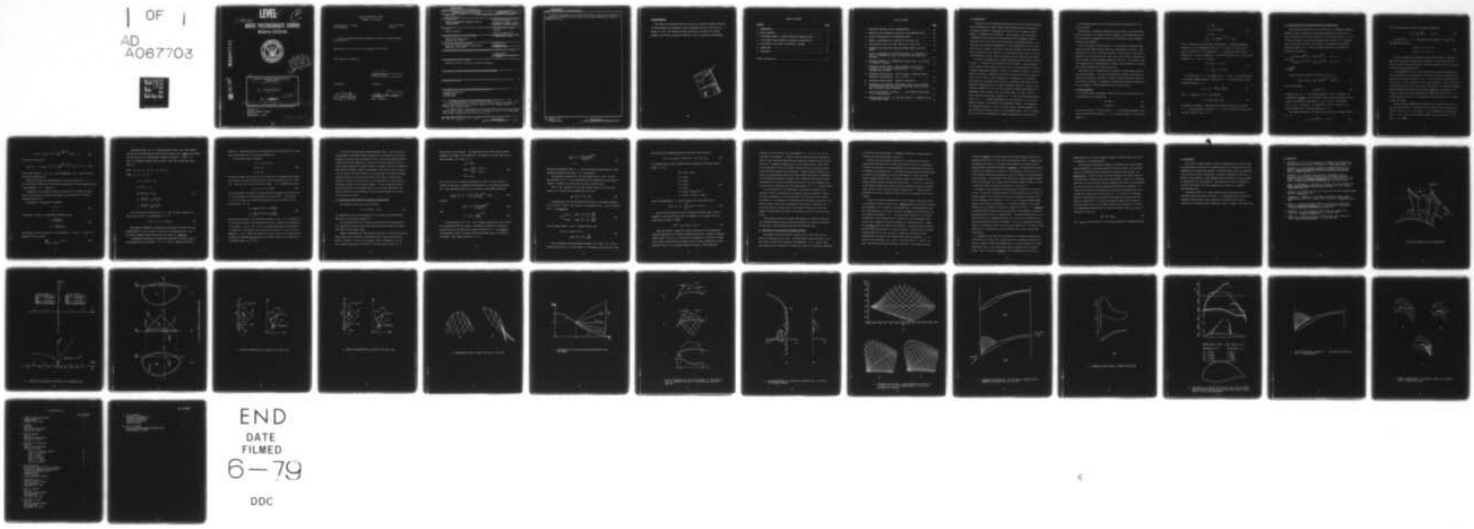

END
DATE FILMED
6-79
DDC

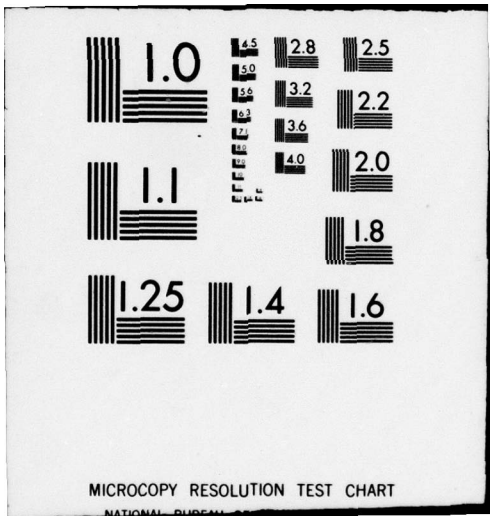
1.0
1.1
1.25
1.4
1.6
1.8
2.0
2.2
2.5
2.8
3.2
3.6
4.0
4.5
5.0
5.6
6.3
MICROCOPY RESOLUTION TEST CHART

LEVEL

(14) NPS67-78-005

NAVAL POSTGRADUATE SCHOOL

Monterey, California

(6) DESIGN OF SHOCK-FREE TRANSONIC FLOW IN TURBOMACHINERY

(10) Helmut/Sobieczky

(12) 41 p.

(11) Nov[redacted]78

(9) Technical rept. 24 Jun - 15 Aug 78,

Prepared for:
Naval Air Systems Command
Code AIR-310
Washington, DC 20360

NAVAL POSTGRADUATE SCHOOL

Monterey, California

Rear Admiral T. F. Dedman
Superintendent

Jack R. Borsting
Provost

The work reported herein was supported by Naval Air Systems Command, Washington, DC.

This report was prepared by:

HELMUT SOBIECZKY
Visiting Professor of Aeronautics

Reviewed by:

M. F. PLATZER, Chairman
Department of Aeronautics

Released by:

W. M. TOLLES
Dean of Research

UNCLASSIFIED

SECURITY CLASSIFICATION OF THIS PAGE (When Data Entered)

REPORT DOCUMENTATION PAGE		READ INSTRUCTIONS BEFORE COMPLETING FORM
1. REPORT NUMBER NPS-67-78-005	2. GOVT ACCESSION NO.	3. RECIPIENT'S CATALOG NUMBER
4. TITLE (and Subtitle) DESIGN OF SHOCK-FREE TRANSONIC FLOW IN TURBOMACHINERY		5. TYPE OF REPORT & PERIOD COVERED Technical Report 20 June-15 August 1978 6. PERFORMING ORG. REPORT NUMBER
7. AUTHOR(s) Helmut Sobieczky		8. CONTRACT OR GRANT NUMBER(s) 61153N; N00019-78-WR-81002
9. PERFORMING ORGANIZATION NAME AND ADDRESS Naval Postgraduate School Monterey, CA 93940		10. PROGRAM ELEMENT, PROJECT, TASK AREA & WORK UNIT NUMBERS
11. CONTROLLING OFFICE NAME AND ADDRESS Naval Air Systems Command, Code AIR-310 Washington, DC 20360		12. REPORT DATE November 1978 13. NUMBER OF PAGES
14. MONITORING AGENCY NAME & ADDRESS(if different from Controlling Office)		15. SECURITY CLASS. (of this report) UNCLASSIFIED 15a. DECLASSIFICATION/DOWNGRADING SCHEDULE

16. DISTRIBUTION STATEMENT (of this Report)

Approved for public release, distribution unlimited

17. DISTRIBUTION STATEMENT (of the abstract entered in Block 20, if different from Report)

18. SUPPLEMENTARY NOTES

19. KEY WORDS (Continue on reverse side if necessary and identify by block number)

Transonic Aerodynamics
Turbomachinery
Cascade Flows

20. ABSTRACT (Continue on reverse side if necessary and identify by block number)

A new design method for transonic flow in turbomachinery is described. The idea is based on the author's previous experience with hodograph methods but carried out in physical space.

If combined with a flow analysis code the new method can be used as a design/analysis tool. Results illustrating this procedure are given for two dimensional flow through cascades and past airfoils. → over

DD FORM 1473 EDITION OF NOV 65 IS OBSOLETE
S/N 0102-014-6601

UNCLASSIFIED
SECURITY CLASSIFICATION OF THIS PAGE (When Data Entered)

Existing configurations can be made shock-free by computational modifications which are limited to that portion of the design shape which is wetted by supersonic flow.

Acknowledgements

This report was prepared while the author was a Visiting Research Professor in the Department of Aeronautics, Naval Postgraduate School, from June 20 to August 15, 1978. The financial support provided by the Naval Air Systems Command, Code AIR-310, under Work Order No. 57236 is gratefully acknowledged.

TABLE OF CONTENTS

LIST OF FIGURES

1. Introduction

Transonic flow in turbomachinery has become a field of increasing interest since requirements for higher engine thrust-to-weight ratios have forced the operating conditions of compressors and turbines into the regime of mixed subsonic - supersonic flow conditions. Since transonic flows are usually accompanied by shock waves which may adversely effect compressor/turbine efficiency due to wave drag, viscous interactions and unsteady effects, it is important for the design aerodynamicist to have computational tools for transonic airfoil-, cascade-, and channel flows which minimize the shock effects. This is analogous to the situation in aircraft design where tools for wing and body definition to obtain shapes with minimal drag for given lift are needed.

The flow in turbomachinery is usually unsteady because of blade row interactions. In addition, viscous effects are often present. Current analyses usually neglect these effects in order to arrive at models which are tractable by current computational methods. Hence, if we restrict our model to inviscid, steady, irrotational compressible flow past a blade row as shown in Figure 1, then we have at least a clear formulation of a defined goal: we intend to give shapes for the blades which will lead to shock-free flow with the above described idealizations and for special operating conditions. Figure 1 is an "artist's concept" of a flow with local supersonic regions and isentropic recompression; sonic surfaces with a local Mach number M equal to One are drawn, dividing the supersonic regions $(M > 1)$ from the surrounding subsonic field $(M < 1)$. A further idealization is the investigation of plane flow examples instead of the sketched three-dimensional problem. The unwrapping of cylindrical sections of a rotor or stator leads to infinite sequences of the airfoil-like blade sections in a two-dimensional plane. This - in comparison to real flow in turbomachinery - modest configuration is our goal here.

The following chapter will introduce the usual basic equations for this type of problem.

Following this a hodograph transformation and a method of characteristics will be presented. This chapter serves to explain a new mathematical principle for mixed flow computation, which was first applied to solve hodograph boundary value problems.

In the next chapter a direct method in the flow plane is developed using a more physically defined model rather than a mathematical principle. Both approaches are, in fact, identical procedures, but the latter direct method certainly will have more practical value, since a high amount of experience is usually needed to operate hodograph methods in practice. Nevertheless, important insight into and understanding of transonic flow phenomena may be gained from indirect methods and problem formulations.

The presentation of design methods is followed by some examples obtained with these techniques. The direct design method is already operational for aircraft wing sections, therefore an example of direct shock-free single airfoil design is included. Development of single airfoil design procedures but also an extension to three-dimensional flows is given in Ref. 1.

2. Basic Equations

We consider steady compressible isentropic flow with the basic relations of continuity and irrotationality:

$$\operatorname{div}(\rho\vec{w}) = 0 \tag{1a}$$

$$\operatorname{rot}(\vec{w}) = 0 \tag{1b}$$

with the flow vector $\vec{w}$ and the density ρ. The wellknown gasdynamic relations for isentropic flow define ρ, w, the speed of sound a and the Mach number M:

$$w = |\vec{w}|$$

$$a^2 = a_o^2 - \frac{\gamma-1}{2} w^2 \qquad (2)$$

$$M = w/a$$

$$\rho/\rho_o = (1 + \frac{\gamma-1}{2} M^2)^{-1/\gamma-1} = F(M)$$

with γ the ratio of specific heats and subscript o defining stagnation conditions. For two-dimensional flow in an x, y-plane the relation (1a) permits introduction of a streamfunction ψ ; irrotationality (1b) allows definition of a velocity potential ϕ , with its gradients equal to the velocity components in x- and y- direction:

$$\phi_x = \frac{1}{\rho} \psi_y = u = w \cos\delta$$

$$\phi_y = -\frac{1}{\rho} \psi_x = v = w \sin\delta \qquad (3)$$

The flow angle is δ . The system (3) for ϕ and ψ is a generalization of the Cauchy-Riemann equations, elimination of ψ by differentiation yields a Poisson equation for ϕ :

$$\phi_{xx} + \phi_{yy} = -(\frac{\rho_x}{\rho} \phi_x + \frac{\rho_y}{\rho} \phi_y) \qquad (4)$$

with ρ a function (2) of M , and therefore

$$\rho = \rho(w) = \rho(\phi_x^2 + \phi_y^2) \ , \qquad (5)$$

the system is nonlinear. Furthermore, the system is of elliptic type when $M < 1$, and of hyperbolic type when $M > 1$, with a parabolic type line along the sonic velocity locus $M = 1$.

3. An Indirect Method to Compute Shock-Free Transonic Flows

The following transformation into a special kind of hodograph variable is included to gain advantages of the resulting system against equation (4): first, the equations will become linear, but also the sonic locus $M = 1$ will be known in advance so that the type change from an elliptic to a hyperbolic solver routine will not have to be iterated. We introduce a Mach number - dependent variable $\nu(M)$, which is defined differently for subsonic and supersonic Mach numbers:

$$\nu(M) = \begin{cases} C \arctan\left(C\sqrt{M^2-1}\right) - \arctan\sqrt{M^2-1}, & \text{for } M \geq 1 \\ C \operatorname{artanh}\left(C\sqrt{1-M^2}\right) - \operatorname{artanh}\sqrt{1-M^2}, & \text{for } M \leq 1 \end{cases} \tag{6}$$

$$C = \left(\frac{\gamma+1}{\gamma-1}\right)^{1/2} .$$

Another variable used in the following relations is

$$K(M) = K(M(\nu)) = \left(1 + \frac{\gamma-1}{2} M^2\right)^{1/\gamma-1} \sqrt{|M^2-1|} . \tag{7}$$

With the flow angle

$$\delta = \arctan {}^{v}/_{u} , \tag{8}$$

a working plane (ν,δ), the socalled Rheograph - plane, is defined. As illustrated in Figure 2, the transformed system (3) in the Rheograph plane is linear but different in the supersonic $(\nu \geq 0 , M \geq 1)$ and subsonic $(\nu \leq 0 , M \leq 1)$ half-plane. The coefficient $K(\nu)$ is positive, with a weakly singular zero at the sonic condition $\nu = 0$.

The system for subsonic flow gives a linear (elliptic) Poisson equation for ϕ.

$$\phi_{\nu\nu} + \phi_{\delta\delta} = \frac{K_\nu}{K} \phi_\nu , \quad (\nu \leq 0) , \tag{9}$$

and a linear hyperbolic system for supersonic velocities:

$$\phi_{\nu\nu} - \phi_{\delta\delta} = \frac{K_\nu}{K} \phi_\nu \qquad (\nu \geq 0) \; ; \tag{10}$$

The sonic locus $\nu = 0$ is included in both systems as a contact line with common sonic values

$$\begin{aligned} \phi^*(\delta) &= \phi \; (\nu \to \pm 0 \; , \; \delta) \; , \\ \psi^*(\delta) &= \psi \; (\nu \to \pm 0 \; , \; \delta) \; . \end{aligned} \tag{11}$$

In order to obtain any solution with these common values we will have to solve the two systems in some suitable coupled way. This seems difficult, but the following simple idea allows a decoupled computation, which will prove effective for design computations.

A flow example with a local supersonic region embedded in subsonic flow can be obtained in the following way. At first we will solve a boundary value problem for the elliptic system $(\nu \leq 0)$ in order to get the subsonic part of the flow and to obtain proper sonic line values along the δ- axis. The latter is effectively carried out by an analytic continuation of the elliptic boundary value problem into the hyperbolic halfplane, Figure 3a, and solution of the elliptic system within these boundaries; the hyperbolic system (10) for $\nu > 0$ is made elliptic like (9) in the continuation region, temporarily by a simple change of one sign.

Assume we found a computational solution for this problem by use of an elliptic solver routine. The solution will be valid for local subsonic flow, values $\phi^*(\delta) = \phi(0 \; , \; \delta)$ are avila le. A local expansion of the solution near $\nu \sim (-0)$ by use of the system in figure 2 and the structure of $K(\nu)$ near $\nu \sim 0$, namely

$$K^*(\nu) = c|\nu|^{1/3} = 3^{1/3}\left(\frac{\gamma+1}{2}\right)^{\frac{1}{\gamma-1}+\frac{1}{3}}|\nu|^{1/3} + \ldots , \qquad (12)$$

has to have the structure

$$\phi(\nu\sim(-0)\ ,\ \delta) = \phi^*(\delta) + 3^{4/3}\,2^{-2}\left(\frac{\gamma+1}{2}\right)^{\frac{1}{\gamma-1}+\frac{1}{3}}\nu^{4/3}\,\psi_\delta^* + O(\nu^2) \ldots \qquad (13)$$

With a known solution ϕ in $\nu \leq 0$ the streamfunction $\psi^*(\delta)$ along the sonic line can be integrated now.

Thus both potential and streamfunction are known along the line $M = 1$, they form initial conditions for the following integration of the hyperbolic system in the halfplane $\nu > 0$, (Figure 2).

Integration of the hyperbolic system is carried out by a method of characteristics which will be outlined here because of its use also for the direct method described later.

Introduction of characteristic variables

$$\begin{aligned} \xi &= \delta + \nu , \\ \eta &= \delta - \nu \end{aligned} \qquad (14)$$

(see Figure 3b) leads to a transformed hyperbolic system

$$\begin{aligned} \phi_\xi &= K\left(\frac{\xi-\eta}{2}\right)\psi_\xi \\ \phi_\eta &= -K\left(\frac{\xi-\eta}{2}\right)\psi_\eta \end{aligned} \qquad (15)$$

which means, that the inclination of characteristics $\xi = \text{const.}$, $\eta = \text{const.}$ is defined in the ϕ,ψ-plane:

$$\left.\frac{d\psi}{d\phi}\right|_{\xi,\eta = \text{const.}} = \pm K^{-1} \qquad (16)$$

With known values ϕ^* , ψ^* along the initial (sonic) line, this relation (16) allows a marching procedure away from the initial line. Figure 4 illustrates how the solution in an infinitesimal triangle is obtained: ϕ and ψ in point 3 is defined by given values in points 1 and 2 and the averaged coefficient K_m

Given: $\nu_1 = \nu_2$, δ_1 , δ_2 , ϕ_1 , ψ_2 , ϕ_2 , ψ_2 .

Asked: ν_3 , δ_3 , ϕ_3 , ψ_3 .

$$\nu_3 = \nu_1 + \frac{1}{2}(\delta_1 - \delta_2) ,$$

$$\delta_3 = \frac{1}{2}(\delta_1 + \delta_2) ,$$

$$K_m = \frac{1}{2}(K(\nu_1) + K(\nu_3) , \qquad (17)$$

$$\phi_3 = \frac{\phi_1 + \phi_2}{2} + K_m \frac{\psi_1 - \psi_2}{2} ,$$

$$\psi_3 = \frac{\psi_1 + \psi_2}{2} + \frac{1}{K_m} \frac{\phi_1 + \phi_2}{2} .$$

Due to the analytic structure (12) of K near the sonic condition, for sonic initial points 1,2 the averaging of K is

$$K_m\,(\nu_1 = \nu_2 = 0) = \frac{3}{4} K(\nu_3) . \qquad (18)$$

This "sonic" averaging is a discretized description of the fact that the characteristics in the ϕ,ψ-plane, (as well as in the physical plane x,y), have Neil's parabola cusps when they meet the sonic line, Figure 5a.

A mathematically possible, but physically unrealizable solution exists if the characteristics of one family (ξ or η = const.) intersect each other,

Figure 5b. Though being useful for interpretation of shock-formation in a free flow, such solutions do not have much practical use.

For the given initial conditions,

$$\begin{aligned} &\nu^* = 0 \ , \ \delta_A \geq \delta \geq \delta_B : \\ &\phi = \phi^* \ (\delta) \ , \\ &\psi = \psi^* \ (\delta) \end{aligned} \tag{19}$$

the whole triangle ABC, Figure 4a, can be evaluated by a straightforward integration based on (17) using the characteristic grid and marching into the ν-direction. This way, with the starting sonic isotach $\nu = 0$, neighboring isotachs

$$\nu_3 = \nu_1 + \Delta\nu = \nu_1 + \frac{1}{2}\,\Delta\delta \tag{20}$$

can be obtained by this method, a concept which was extended by the author also for the computation of three-dimensional flow fields, Ref. 2. The solution ϕ , ψ (ν, δ) within the triangle ABC defines now also the solution in the physical plane x,y by

$$\begin{aligned} dx &= \frac{1}{w(\nu)} \left(\cos\delta \ d\phi - \sin\delta \ \frac{d\psi}{\rho(\nu)}\right) , \\ dy &= \frac{1}{w(\nu)} \left(\sin\delta \ d\phi + \cos\delta \ \frac{d\psi}{\rho(\nu)}\right) . \end{aligned} \tag{21}$$

particularly the shape of the resulting streamline $\psi(\nu,\delta) = \psi_o$, see Figure 2b, if the elliptic boundary value problem solved before (Figure 3a) was defined by a curve where $\psi = \psi_o = \text{const}$, which is a Neumann type boundary value problem for system (9). In Figure 3c the solutions of the elliptic $(\nu \leq 0)$ and the hyperbolic $(\nu \geq 0)$ region are combined now and, though solved by <u>two</u> different systems, they represent <u>one</u> transonic flow solution, which can be evaluated in the physical plane x,y by (21).

As we know from operational hodograph methods, Refs. 3 and 4, the relations between the hodograph (input) boundaries and the physical flow (output) boundaries resulting from the obtained solution are usually complicated and it requires rather much experience to operate such indirect methods in order to obtain useful examples of transonic airfoils, cascades or other flow boundaries. Some ideas about airfoil design with methods of this type are given in Refs. 5 and 6, here we only want to point out the basic idea of solving an extended elliptic boundary value problem first and use the result to integrate the hyperbolic stystem in the second step. This technique will be used again in the method outlined in the following chapter. It will be explained without using the details of the hodograph method, but the reader undoubtedly will find the same basic idea resulting in strong relations between the indirect and the new direct method.

4. A New Direct Design Method for Transonic Configurations

The isentropic relation (2) for the density

$$\rho/\rho_o = F(M(\phi_x^2 + \phi_y^2)) \tag{22}$$

is responsible for both the nonlinearity of (1) and the elliptic/hyperbolic mixed type of the Poisson equation (4).

The following idea will not remove the nonlinearity of the system but it will establish a uniform elliptic type Poisson equation throughout the whole flow field and Mach number range.

Imagine a modification of the isentropic gas model in the way that the gas might behave like an isentropic compressible gas as long as the local Mach number is subsonic. When the local speed of sound is exceeded in the flow past a given configuration, the density of the gas model is frozen to the

value of sonic flow condition. This means that this fictitious gas is incompressible in supersonic flow conditions! More generally we might think also of other relations $\rho(M)$ when $M \geq 1$:

$$\rho/\rho_o = \tilde{F}(M) :$$

$$\tilde{F}(M) = \begin{cases} F(M) & (M \leq 1) , \\ \bar{F}(M) & (M \geq 1) , \end{cases} \tag{23}$$

$$\bar{F}(1) = F(1)$$

but we have to ask for possible constraints for $\bar{F}(M)$ in order to get an elliptic and not again a hyperbolic system similar to the original isentropic one. This constraint exists and it is defined by the limiting conditions

$$\frac{\rho \cdot w}{\rho_o \cdot a^*} = \bar{F}_L(M) \cdot M \cdot \left(\frac{\gamma + 1}{2 + (\gamma-1)M^2} \right)^{1/2} = \text{const.} \tag{24}$$

yielding

$$\bar{F}_L(M) = F^* \cdot \left(\frac{2 + (\gamma-1)M^2}{(\gamma+1)M^2} \right)^{1/2} \tag{25}$$

with

$$F^* = \rho^*/\rho_o = \left(\frac{2}{\gamma+1} \right)^{1/\gamma-1} . \tag{26}$$

A fictitious gas with $\bar{F} = \bar{F}_L$ in the supersonic region will lead to parabolic equations within this region. This model is therefore a limiting and excluded border of a whole area of possible relations for $\bar{F}$, see Figure 6. A one-parametric family of possible fictitious elliptic gases is defined by the density - Mach number relation for $M \geq 1$

$$\bar{F}_P(M) = F^* \cdot \left(\frac{2 + (\gamma-1)M^2}{(\gamma+1)M^2} \right)^{P/2} , \qquad P < 1 \tag{27}$$

excluding the parabolic limit $P = 1$ and including the above mentioned "incompressible supersonic flow" when $P = 0$, see Figure 6.

The isentropic relation $F(M)$ and the parabolic limit $F_L(M)$ have the same gradient at $M = 1$, thus indicating that the isentropic relation leads to parabolic equations just at the sonic surface in the flow field.

With a $\rho(M)$ relation (23) the basic Poisson equation (4) will be nonlinear but of elliptic type throughout the flow field:

$$\tilde{\phi}_{xx} + \tilde{\phi}_{yy} = \tilde{P} \, (\tilde{\phi}_x , \tilde{\phi}_y) . \tag{28}$$

Corresponding to the real and the fictitious part of the density relation (23), a solution $\tilde{\phi}(x,y)$ will consist of an isentropic part ϕ and a fictitious part $\bar{\phi}$, see Figure 7a :

$$\tilde{\phi} = \begin{cases} \phi(x,y) , & \text{where } \tilde{\phi}_x^{\,2} + \tilde{\phi}_y^{\,2} \leq \dfrac{2a_o^{\,2}}{1+\gamma} \\ \bar{\phi}(x,y) , & \text{where } \tilde{\phi}_x^{\,2} + \tilde{\phi}_y^{\,2} \geq \dfrac{2a_o^{\,2}}{1+\gamma} \end{cases} \tag{29}$$

but with common values ϕ and $\bar{\phi}$ along the sonic line

$$\phi(x^*,y^*) = \bar{\phi}\,(x^*,y^*) = \phi^* , \qquad \text{where } \tilde{\phi}_x^{\,2} + \tilde{\phi}_y^{\,2} = \frac{2a_o^{\,2}}{\gamma+1} \tag{30}$$

From a continuous fictitious density relation (23), namely $F(1) = \bar{F}(1)$, follows that not only $\tilde{\phi}$ but also grad $\tilde{\phi}$ is continuous across the sonic line.

Thus the velocity components along the sonic line may be given by

$$(u^* , v^*) = \text{grad } \phi = \text{grad } \tilde{\phi} \ (x^* , y^*) = (\tilde{\phi}_x , \tilde{\phi}_y) \ . \tag{31}$$

If we define now all sonic condition data as functions of the sonic line arc length s , with

$$\begin{aligned} ds^2 &= dx^{*2} + dy^{*2} \ , \\ x^* &= x^*(s) \ , \\ y^* &= y^*(s) \ , \\ u^* &= u^*(s) \\ v^* &= v^*(s) \ , \\ \delta^* &= \delta^*(s) = \arctan {}^{v^*}/_{u^*} \ , \\ \phi^* &= \phi^*(s) = \tilde{\phi} \ (x^*(s) \ , \ y^*(s)) \ , \end{aligned} \tag{32}$$

then the streamfunction ψ^* along the sonic line follows from (21) to

$$\psi^*(s) = \rho_o \cdot F^* \cdot \int_{s_A=0}^{s} (u^* \dot{y}^* - v^* \dot{x}^*) \, ds \ . \tag{33}$$

With no sources within the local fictitious supersonic region, which is bounded by a wall and the sonic line, see Figure 7a, the integral over the sonic line arc AB has to vanish:

$$\psi^*(0) = \psi^*_A = \psi^*(s_B) = \psi^*_B = 0 \ . \tag{34}$$

This can be used, if needed, to check the accuracy of the conservative numerical algorithm for the elliptic system solved before. Numerical inaccuracy gives a result $\psi^*_B \neq \psi^*_A$, in which case a refinement of the elliptic computation or some correction should be made in order to obtain conservation of mass implied by (34) up to a sufficient degree of accuracy. This having been

achieved, we have from (32), (33) the variables δ^* , ϕ^* , ψ^* , x^* , y^* as functions of the parameter s which we will now need as initial conditions to solve the real isentropic supersonic flow domain and redefine the wall streamline $\psi_o = 0$ between the points A and B in the physical plane. Since (32), (33) is equivalent to (19), the method of characteristics as described above for the indirect approach can be used again. Figure 7b shows a sketch of the result, the characteristics grid and the new surface shape which is compatible with the computed shock-free transonic flow. Compared to the original shape, the modified one is flatter providing more space for the real supersonic flow to pass than the fictitious flow with higher density ($\bar{F} > F$!) required before.

It can be shown that the streamlines of the obtained hyperbolic flow solution fit into the subsonic flow with smooth slope and curvature. This is, of course, important for the practical value of the obtained new wall shape, see Figure 7c. The possibility of obtaining limit lines was illustrated in the previous chapter, Figure 5b; the mentioned restrictions for practical use of such results apply of course also to the approach outlined here, since the method of characteristics is used in the indirect as well as in the new direct method.

The following chapter will present some examples of shock-free transonic flow through cascades and past airfoils obtained with the indirect (hodograph) and the direct design technique which were both discribed here.

5. Application to the Design of Transonic Cascades

The indirect method described in chapter 3 was at first carried out by means of an analog elliptic solver. The rheoelectric analogy was used to solve the elliptic boundary value problem in the Rheograph (ν,δ-) working plane. This analogy has the advantage of a physically clear and illustrative formulation

of the type of problems studied. A systematic technique of obtaining supercritical airfoils was developed, see Ref. 6.

Despite interesting results which led to the development of practical supercritical wing sections, the method could hardly be put into operation on a broader scale because of the electromechanical work involved with the set-up of boundaries, measurement, etc. The analogy has been successful in many fields not only in fluid mechanics but the fast development of larger and faster digital computers opened other, and in many respects more preferable, ways to compute problems where the analogy has served before. For use on a wider scale in the aircraft industry the analog set-up was, therefore, replaced by computational elliptic solver routines like panel methods, Ref. 7. The most recent development is the use of the fast Poisson solver for the elliptic part of the problem.

A result of this more economical way by using numerical techniques instead of the analogy is shown in Figures 8-11. Figure 8a depicts the elliptic boundary value problem in the ν,δ-plane , with singularities, a second Riemann's sheet and a branch-point, but also with an elliptic continuation region reaching into the hyperbolic half-plane $\nu > 0$. The complicated structure of the elliptic boundary will not be discussed here, it defines the resulting physical flow. In this case a compressor cascade was designed, as illustrated below. Figure 8b and Figure 9 show the results of the hyperbolic computation using the method of characteristics described in a previous chapter. In Figure 9a the resulting characteristics grid in the ϕ,ψ-plane is drawn, in Figure 9b the same characteristics are shown in the physical plane with the streamline $\psi_o = 0$. In Figure 9c the isotachs $\nu(M) = \text{const.}$ and the isoclines $\delta = \text{const.}$ are drawn, thus defining the whole supersonic flow field. The resulting cascade

is drawn in Figure 10, the lower blade is the inviscid design with the local supersonic flow field. It has an open trailing edge to allow a boundary layer displacement subtraction. A boundary layer computation was made using the design pressure distribution depicted in Figure 11. The resulting actual blade is shown in the upper part of Figure 10. The pressure on the rear part of the blade follows a Stratford distribution, which is favorable in avoiding boundary layer separation. The thickness of this blade has a minimum somewhat upstream of the trailing edge, which results from the chosen elliptic boundary in order to obtain this type of pressure distribution, see also Ref. 8.

The example of this compressor cascade design was obtained by the indirect method. As outlined, the direct approach has the advantage that an airfoil- or cascade- geometry can be chosen and only the part wetted by supersonic flow will be modified by the algorithm. In Ref. 1 a new combined analysis/design method for 2D airfoils is described. It is based on Jameson's circle plane computer code for analysis of airfoils in transonic flow, Ref. 9. In Figure 12 a conventional NACA 64A410 section was modified by this procedure in order to obtain shock-free flow past a single airfoil. The pressure distribution on the NACA airfoil (with a recompression shock) and on the airfoil obtained by the design procedure (shock-free) are compared. Little lift change and vanishing drag are the practical results of this inviscid computation. Of course, viscous effects can be introduced here also by starting with an open trailing edge airfoil shape.

In a magnified scale the airfoil geometries are compared illustrating the "shave-off" on the upper side. Similar results for compressor cascades like the one in Figure 10 could be obtained also by the direct method if the input blade were thicker in the region which came out supersonic by the indirect method. This is sketched in Figure 13. The implementation of the direct

design method into a cascade computer program is currently under way and will be reported in a forthcoming paper.

A final remark concerning the design of accelerated flow turbine blades should be made here: the indirect method was used for design of the transonic inlet of a cascade with flow accelerated to supersonic exit velocity, see Figure 14 b,c. A result of this type can be obtained by the direct method if the chosen input cascade does not have closed blades, Figure 14a. Streamline contraction of the fictitious "elliptic supersonic flow" due to blade displacement will provide the necessary acceleration through sonic conditions. In Figure 14b the method of characteristics starting at the computed sonic line provides the transonic part of the field $M > 1$, and finally a continuing method of characteristics using data on the limiting characteristic BC and given wall geometry BT", CT' closes the designed cascade blade, Figure 14c. Here the contour part AC of the blade is given by the algorithm. Of course, the streamfunction distribution ψ^* may not have equal values ψ^*_A, ψ^*_B, as postulated in (34), but

$$\psi^*_B - \psi^*_A = \Delta\psi_{casc} \tag{35}$$

with $\Delta\psi_{casc}$ being the amount of flow passing between two neighboring blades.

6. Conclusions

A new idea to compute transonic flows in turbomachinery has been outlined and demonstrated as the basis for computational codes to obtain shock-free flow boundaries like airfoils and cascades. An indirect method, which was developed first, served to outline the principle of elliptic continuation as well as a method of characteristics. Both techniques were then used in a direct approach to design shock-free configurations. This method can be used in combination with any flow analysis code thus extending such a program to a combined analysis/design tool.

Conventional airfoil or cascade geometries can be made shock-free by relatively small alterations of the shape. In combination with a viscous displacement concept boundary layer effects may be included and will not be complicated for design operating conditions by shock - boundary layer interaction.

7. References

1. Sobieczky, H., N. J. Yu, K-Y. Fung and A. R. Seebass, "A New Method for Designing Shock-Free Transonic Configurations," AIAA Paper 78-1114. 1978.

2. Sobieczky, H., "A Computational Algorithm for Embedded Supersonic Flow Domains," University of Arizona Engineering Experiment Station Report, Tucson, Arizona, July 1978.

3. Boerstoel, J. W., "Review of the Application of Hodograph Theory to Transonic Airfoil Design and Theoretical and Experimental Analysis of Shock-Free Airfoils," Symposium Transsonicum II, K. Oswatitsch and D. Rues (Eds.), Springer-Verlag, Berlin, Heidelberg, New York, 1976, 109-133.

4. Bauer, F., Garabedian, P., and Korn, D., "Supercritical Wing Sections III," Lecture Notes in Economics and Mathematical Systems, Vol. 150, Springer-Verlag, New York, 1977.

5. Sobieczky, H., "Entwurf überkritischer Profile mit Hilfe der rheoelektrischen Analogie," DLR-FB 75-43, 1975.

6. Sobieczky, H., Stanewsky, E., "The Design of Transonic Airfoils Under Consideration of Shock Wave Boundary Layer Interaction," ICAS paper 76-14, 1976.

7. Eberle, A., "An Exact Hodograph Method for the Design of Supercritical Sections," Symposium Transsonicum II, K. Oswatitsch and D. Rues (Eds.), Springer-Verlag, Berlin, Heidelberg, New York, 1976.

8. Garabedian, P., "On the Design of Airfoils Having no Boundary Layer Separation," Advances in Mathematics 15, p. 164-168. 1975.

9. Jameson, A., "Iterative Solution of Transonic Flows Over Airfoils and Wings," Comm. Pure and Appl. Math. 27, p. 283-309, 1974.

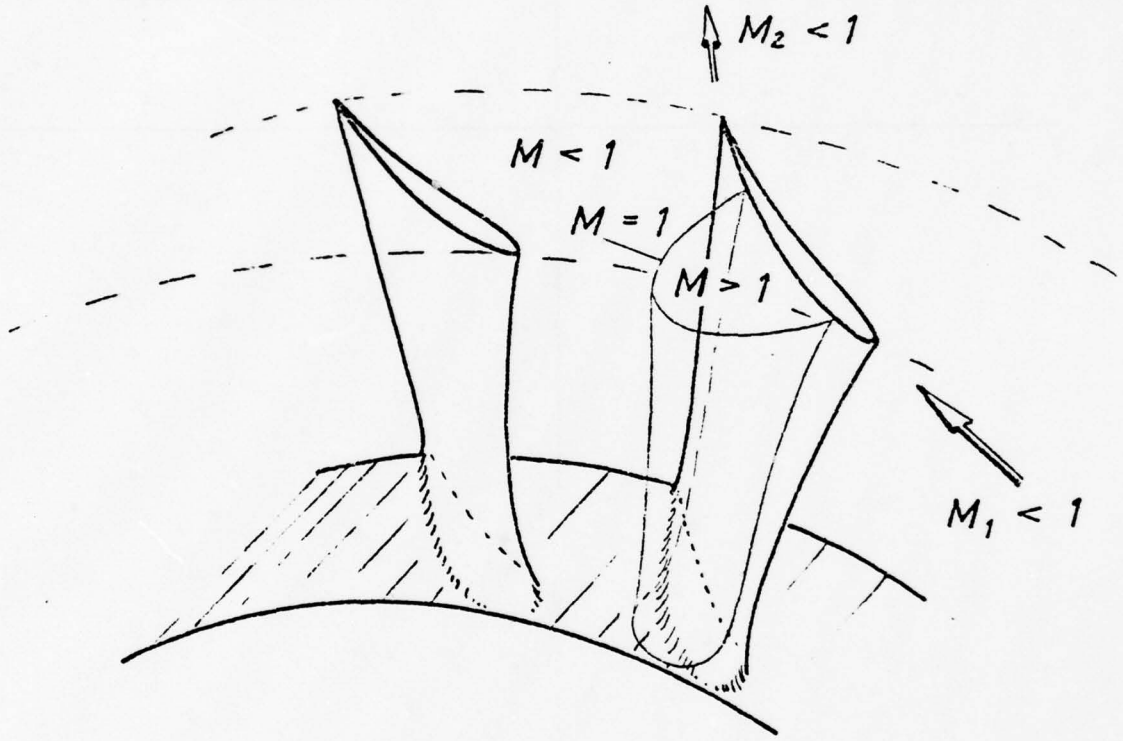

1. SHOCK-FREE TRANSONIC FLOW IN TURBOMACHINERY

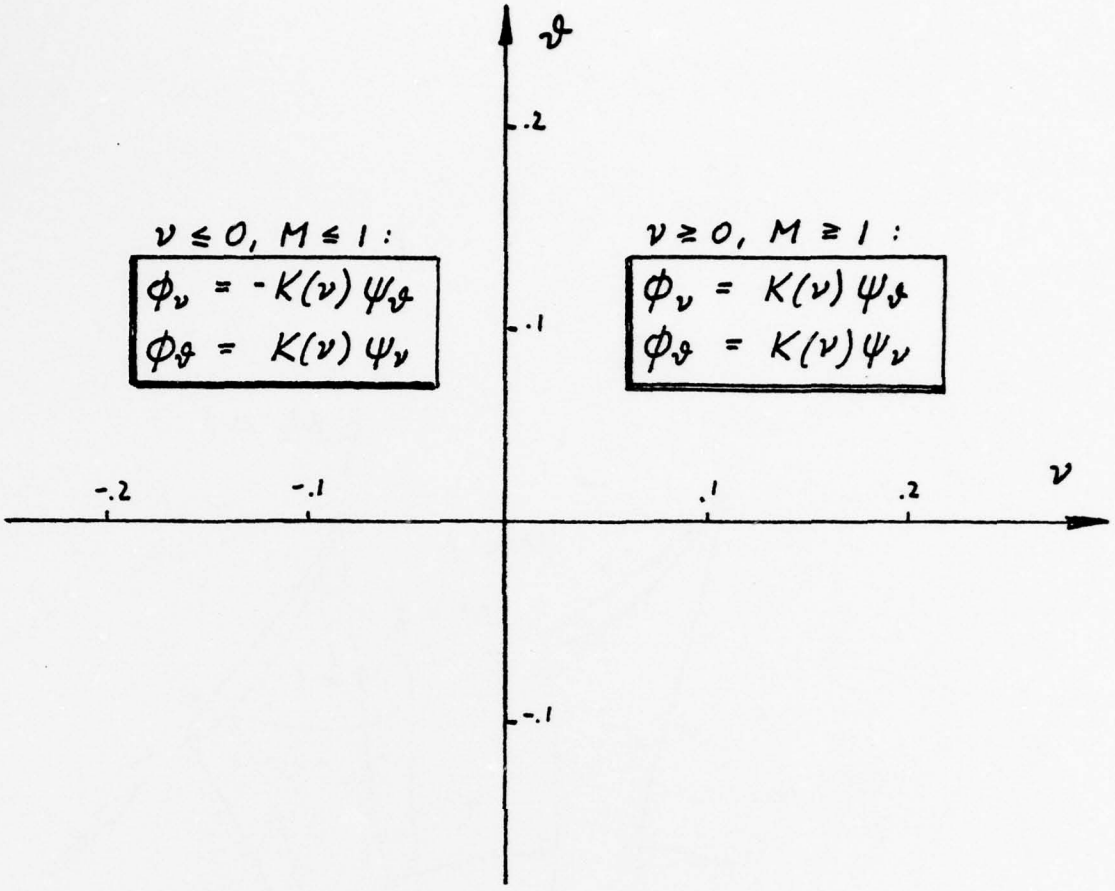

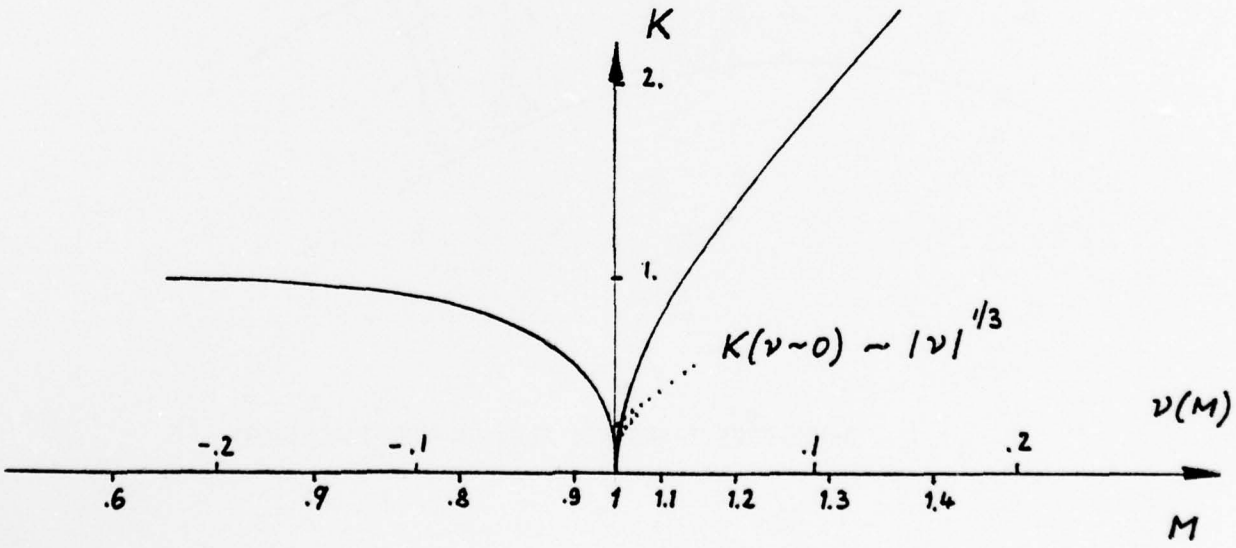

2. POTENTIAL FLOW DIFFERENTIAL EQUATIONS IN THE RHEOGRAPH PLANE

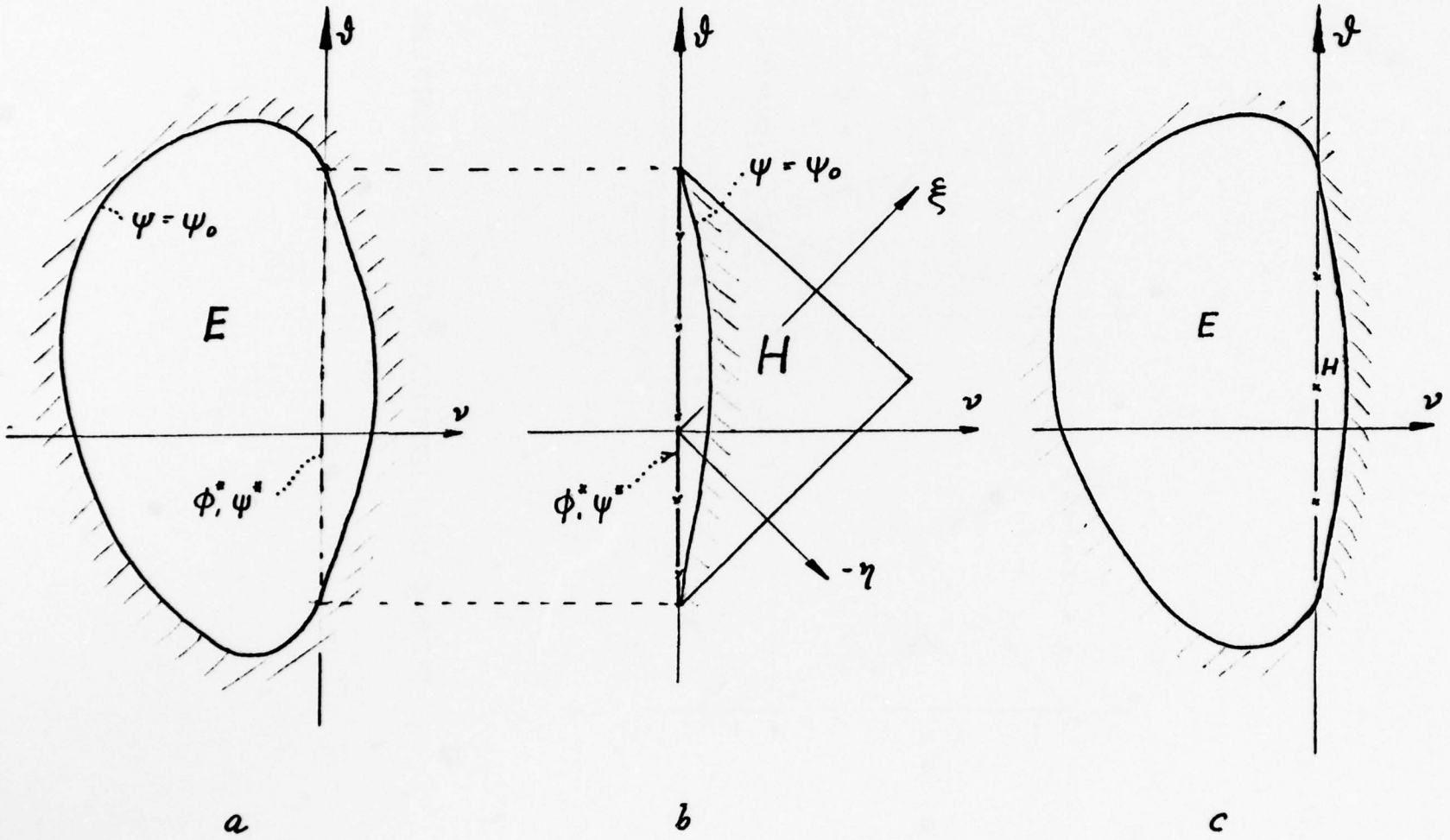

3. ELLIPTIC CONTINUATION IN THE RHEOGRAPH PLANE

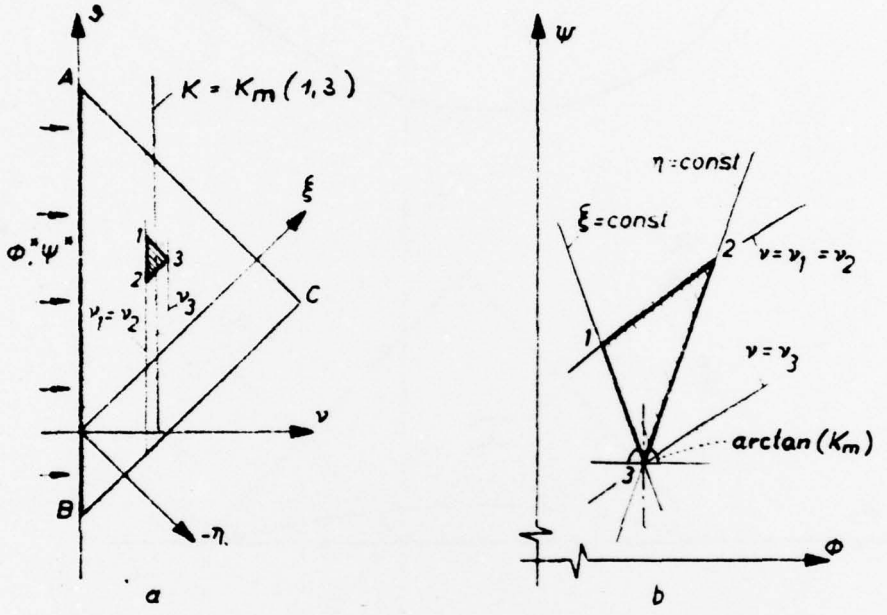

4. METHOD OF CHARACTERISTICS, STARTING AT THE SONIC LINE

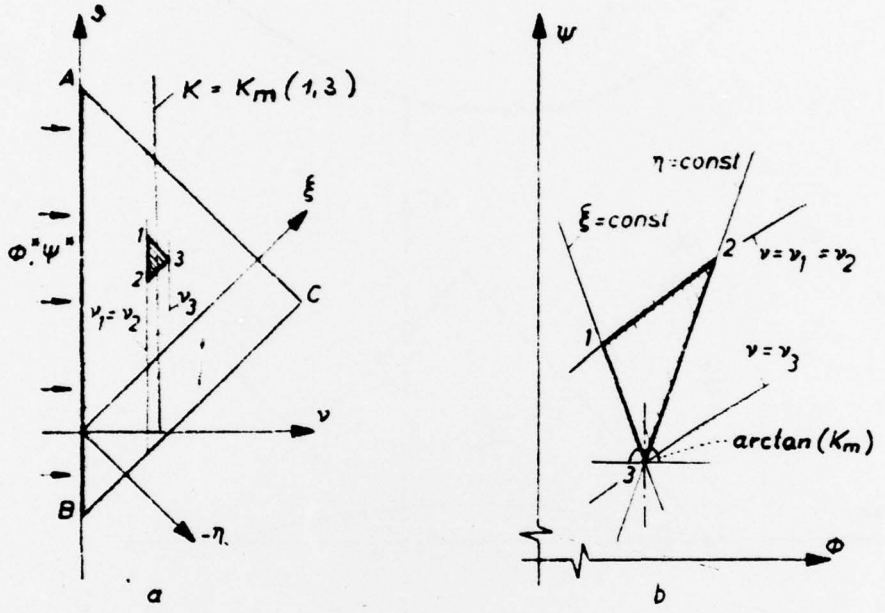

4. METHOD OF CHARACTERISTICS, STARTING AT THE SONIC LINE

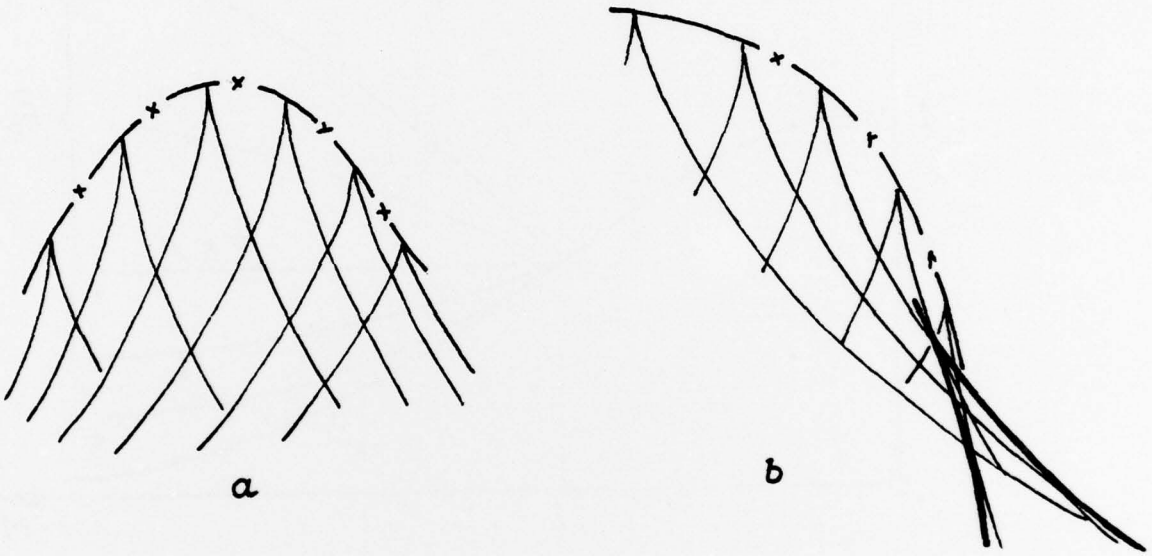

5. CHARACTERISTICS NEAR (a) SONIC LINE AND (b) LIMIT LINE

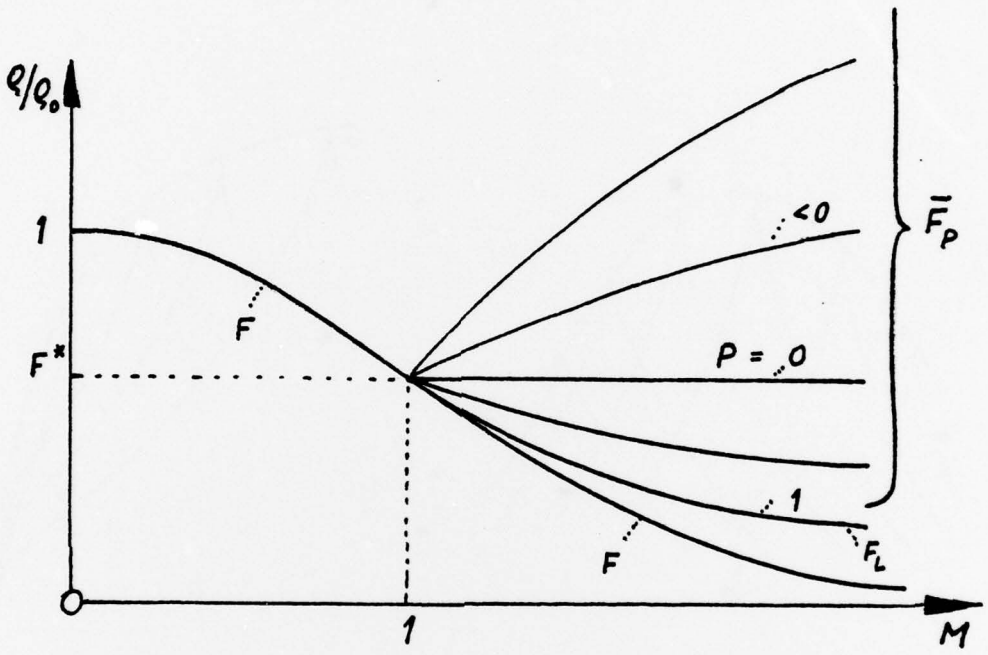

6. ISENTROPIC AND FICTITIOUS RELATIONS BETWEEN DENSITY AND MACH NUMBER

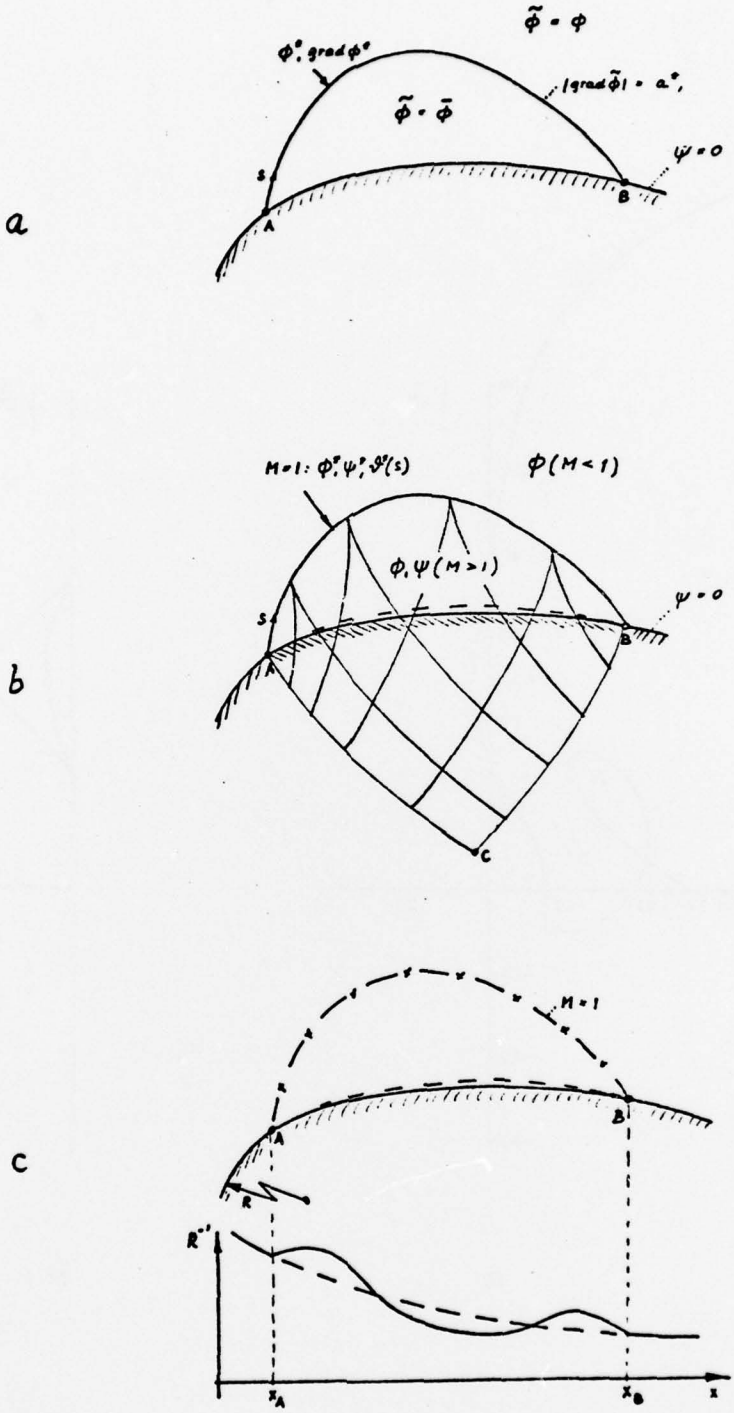

7. ELLIPTIC CONTINUATION IN THE PHYSICAL PLANE: (a) FICTITIOUS GAS FLOW; (b) ISENTROPIC GAS FLOW; (c) RESULTING WALL SHAPE WITH CURVATURE

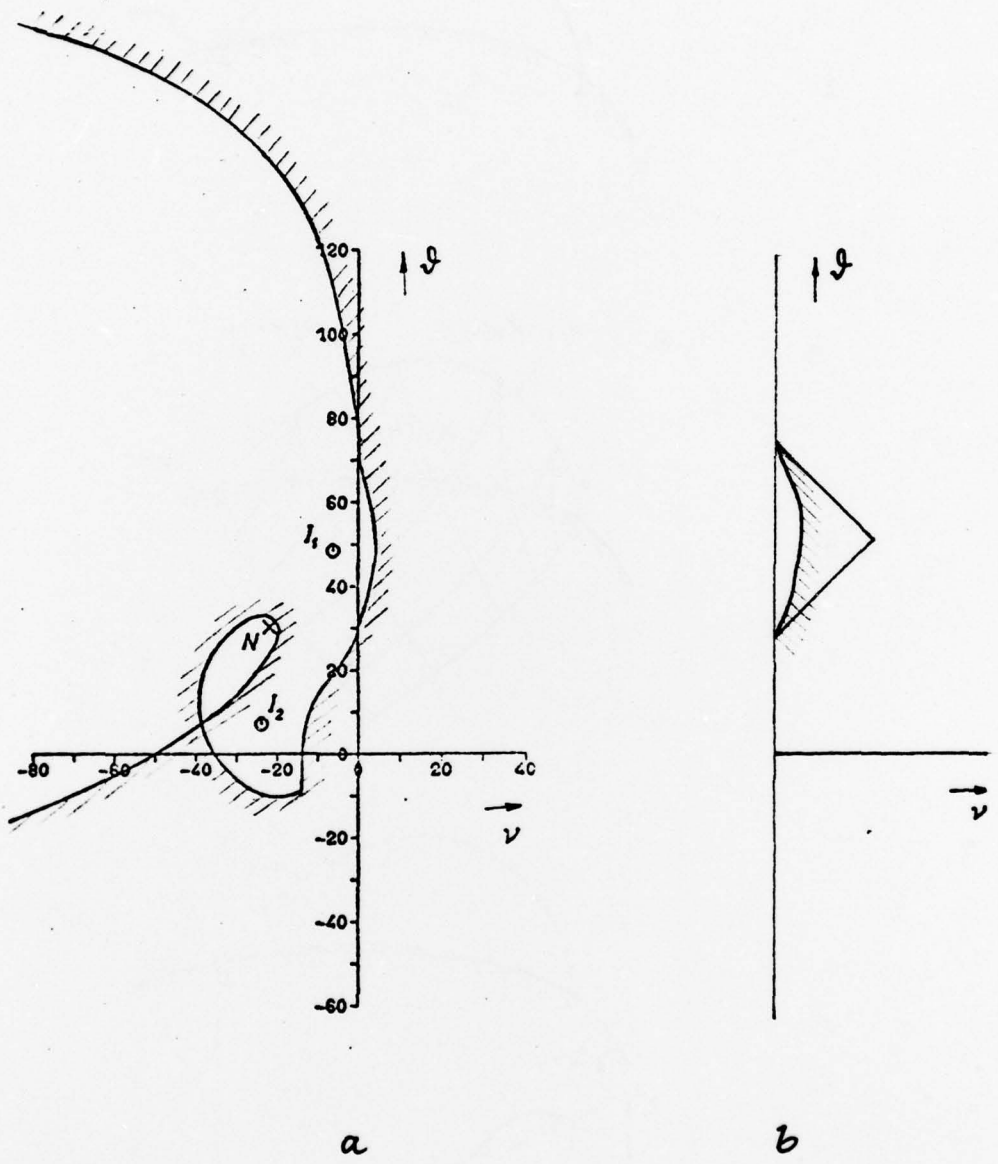

8. RHEOGRAPH BOUNDARY OF A SUPERCRITICAL CASCADE FLOW: (a) ELLIPTIC; (b) HYPERBOLIC PROBLEM

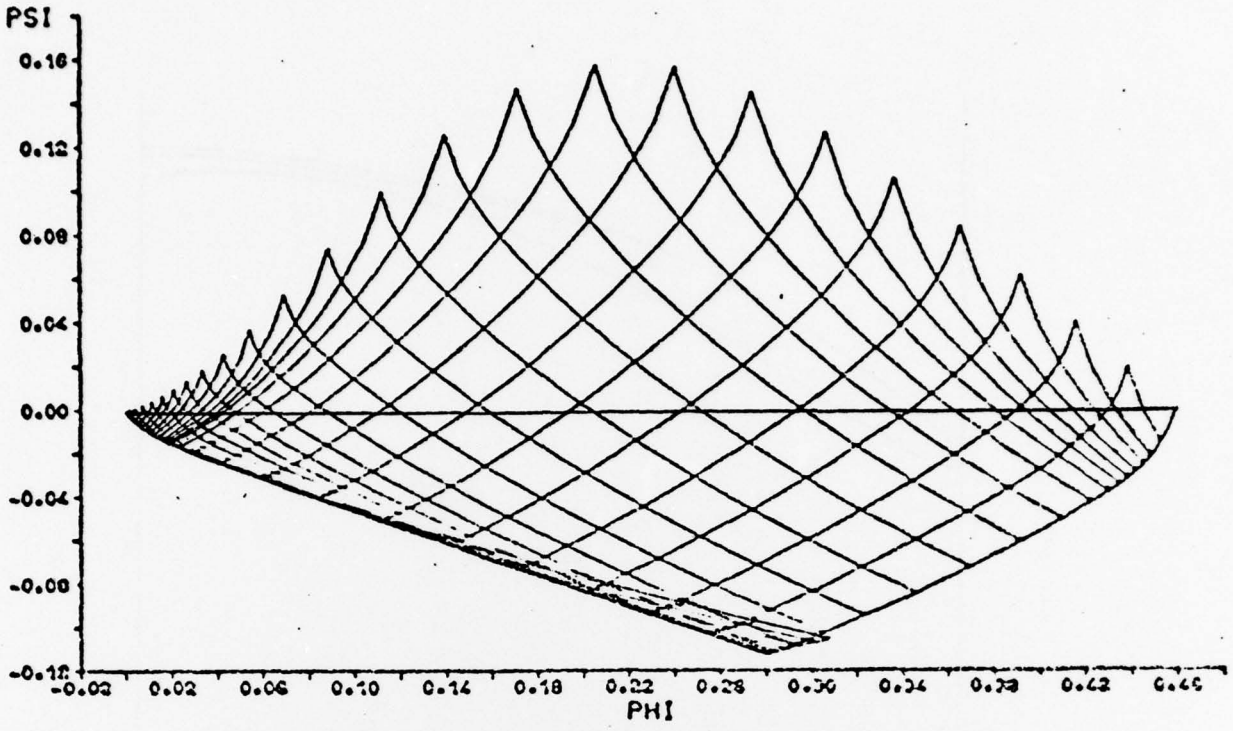

a

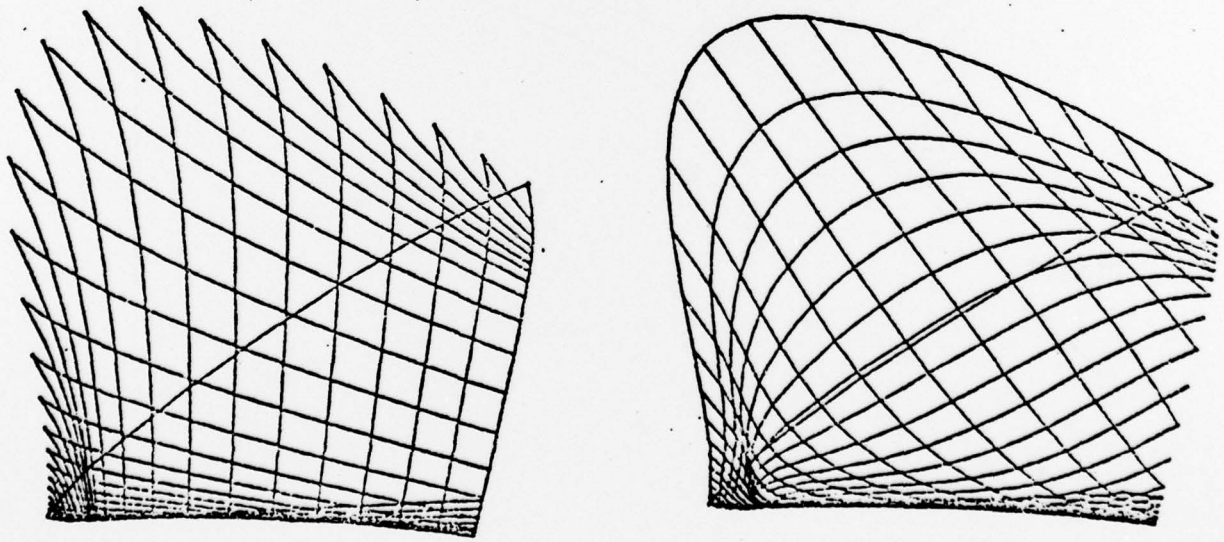

b

c

9. COMPRESSOR CASCADE DESIGN: LOCAL SUPERSONIC FLOW FIELD (a) ϕ,ψ-plane, (b) x,y-plane (CHARACTERISTICS), (c) x,y-plane (ISOTACHS AND ISOCLINES)

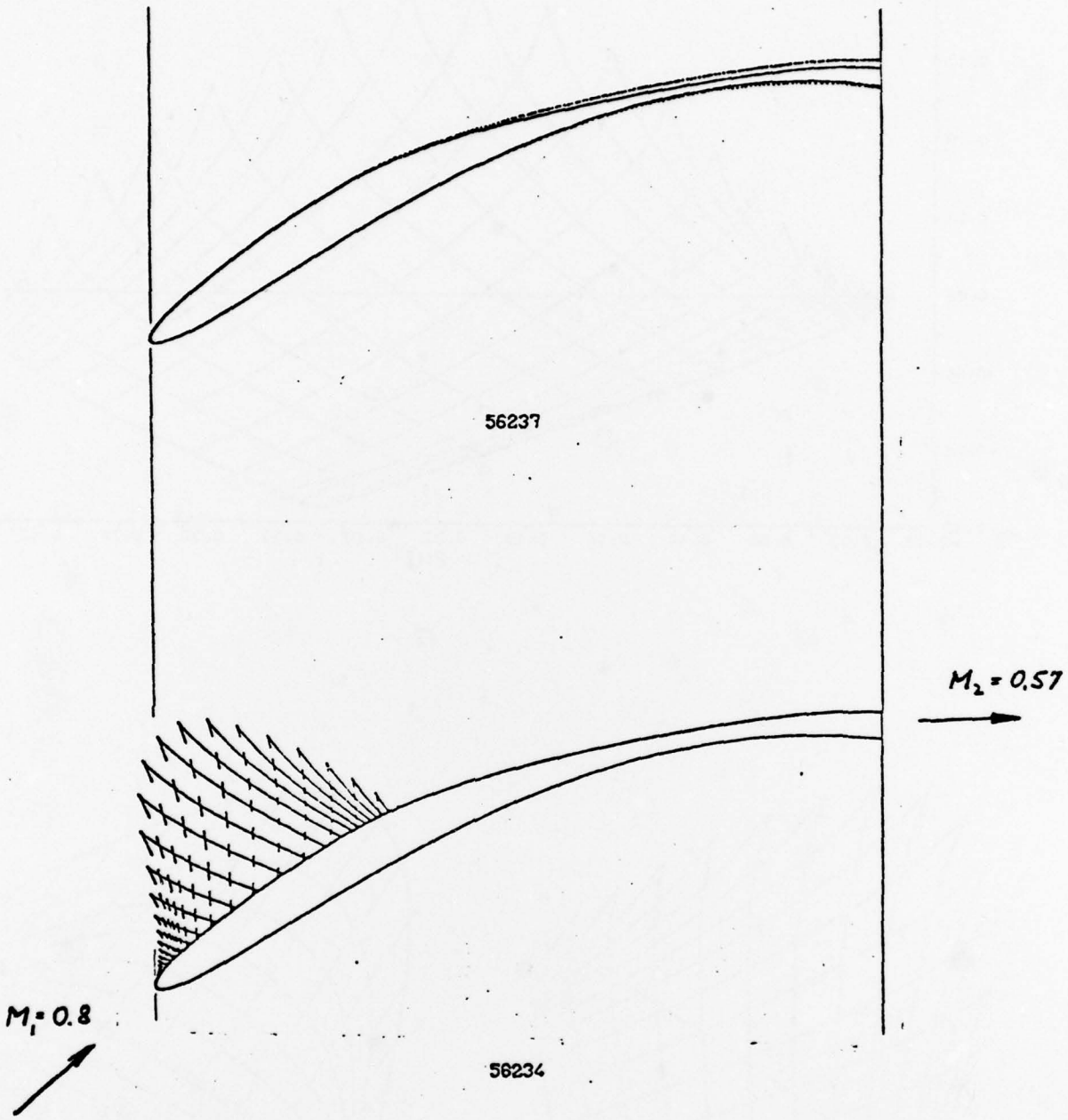

10. COMPRESSOR CASCADE DESIGN: INVISCID DESIGN, SUPERSONIC REGION, BOUNDARY LAYER SUBTRACTION ($Re = 1{,}6.10^6$)

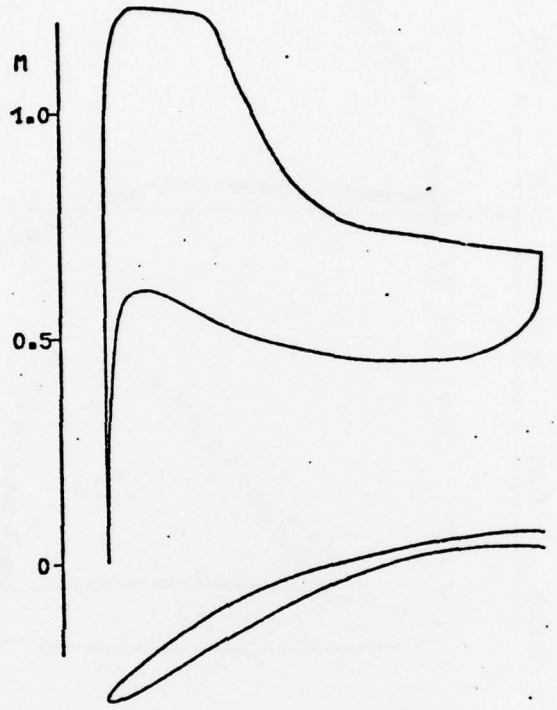

56234

11. COMPRESSOR CASCADE DESIGN: PRESSURE DISTRIBUTION

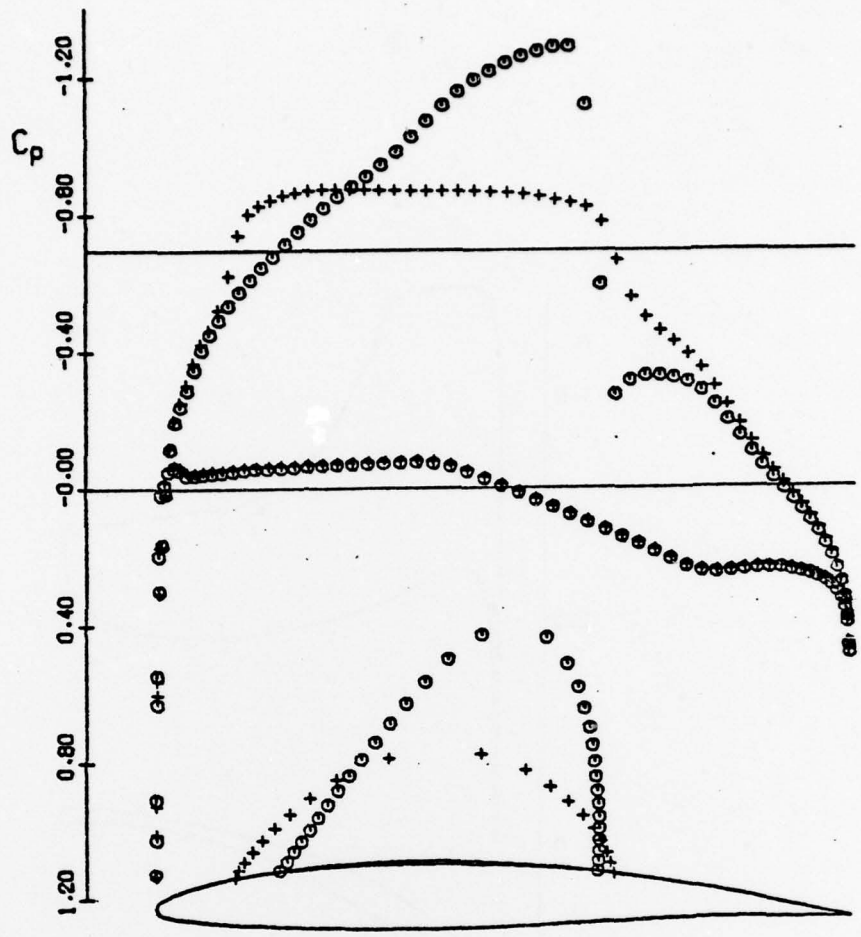

12. COMPARISON OF THE PRESSURE COEFFICIENTS, SONIC LINES AND SHAPES FOR THE BASELINE NACA 64A410 AND THE SHOCK-FREE AIRFOIL OBTAINED FROM IT BY THE 2D DESIGN PROCEDURE

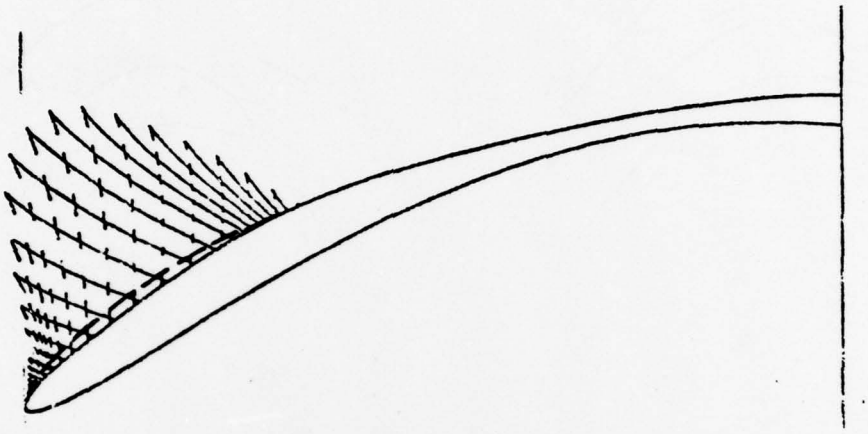

13. DIRECT DESIGN METHOD: ORIGINAL (- - -), AND RESULTING SHOCK-FREE (————) CASCADE DESIGN

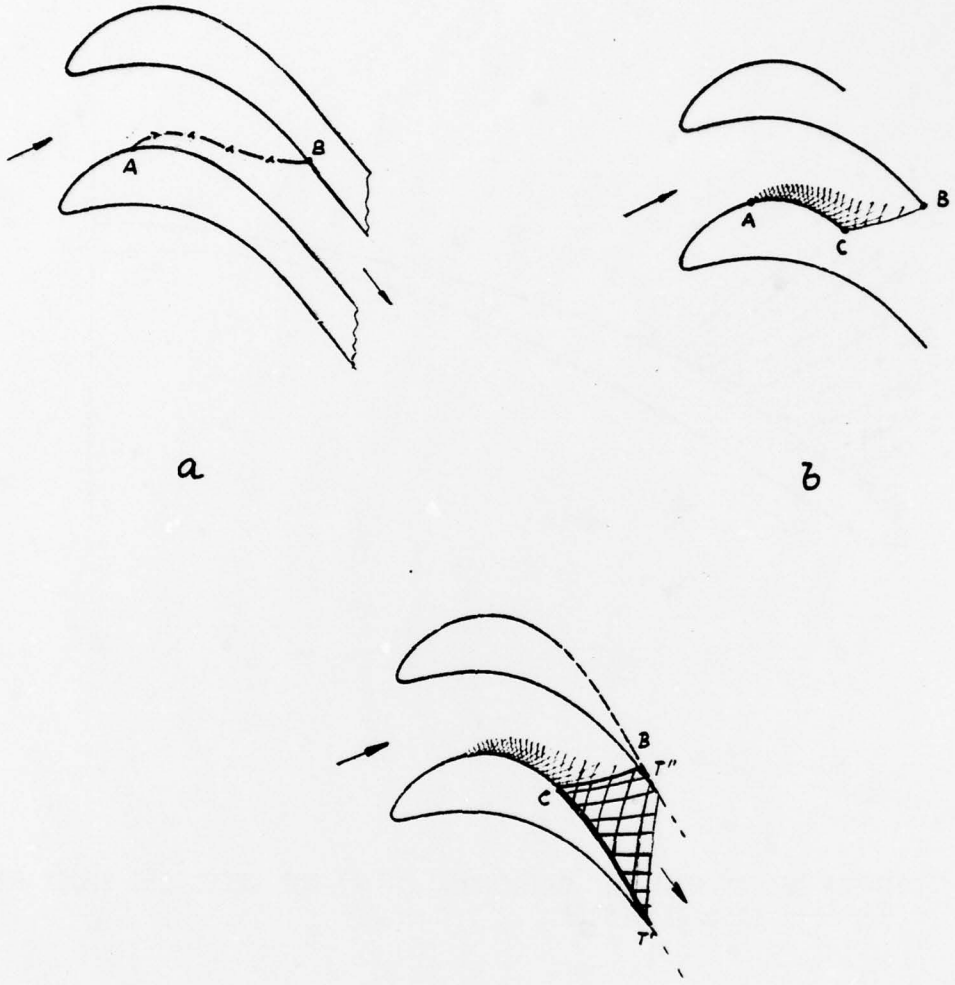

14. TURBINE CASCADE DESIGN: (a) ORIGINAL CASCADE, (b) TRANSONIC INLET, (c) RESULTING CASCADE

Distribution List

		No. of Copies
1.	Defense Documentation Center Cameron Station Alexandria, VA 22314	2
2.	Library Code 0212 Naval Postgraduate School Monterey, CA 93940	2
3.	Dean of Research Code 023 Naval Postgraduate School Monterey, CA 93940	1
4.	Department of Aeronautics Code 67 Naval Postgraduate School Monterey, CA 93940	
	Prof. M. F. Platzer, Chairman	20
	Prof. R. P. Shreeve	1
	Prof. D. Adler	1
	Prof. O. Biblarz	1
	Prof. T. H. Gawain	1
	Prof. D. J. Collins	1
	Prof. D. W. Netzer	1
5.	Dr. H. Sobieczky Institute for Theoretical Fluid Mechanics Deutsche Forschungs-und Versuchsanstalt fur Luft-und Raumfahrt, DFVLR Bunsenstrasse 10 D 3400 Goettingen Federal Republic of Germany	2
6.	Commanding Officer Naval Air Systems Command Navy Department Washington, DC 20360	1
7.	Dr. H. J. Mueller Code 310 Naval Air Systems Command Navy Department Washington, DC 20360	
8.	Mr. Karl H. Guttman Code 330 Naval Air Systems Command Navy Department Washington, DC 20360	1

No. of Copies

9. Dr. R. Seebass — 1
Professor of Mechanical &
Aerospace Engineering
University of Arizona
Tucson, AZ 85721

10. Dr. J. R. Casper — 1
United Technologies Research Laboratories
East Hartford, CT 06108